Behav Ecol Sociobiol (2001) 49:220–234 

ORIGINAL ARTICLE

**D.W. Stephens · J.R. Stevens**

# A simple spatially explicit ideal-free distribution: a model and an experiment

Received: 14 June 2000 / Revised: 20 September 2000 / Accepted: 7 October 2000

**Abstract** This investigation presents a simple spatially explicit analysis of the ideal-free distribution. The traditional ideal-free distribution assumes discrete sites with definite boundaries, and predicts how many individuals should occupy each site. In contrast, the present analysis assumes that a forager's gains gradually decline with distance from a site, and asks where in space individuals ought to be. Although many interesting situations may arise, the analysis asks how individuals should position themselves as the distance between two identical sources increases. Nash equilibrium positions should follow a pitchfork pattern as the distance between sites is increased; that is, an individual should maintain a position between two sources when they are close together but should move nearer one of the sources when they are far apart. In addition, the text describes an experimental study that parallels the theoretical analysis. The experiment supports the predicted pitchfork pattern, and provides somewhat weaker support for the predicted differences in "individual" and "paired" pitchforks.

**Keywords** Ideal-free distribution · Spatial models · Foraging · Starling

## Introduction

The ideal-free distribution, or IFD (Fretwell and Lucas 1970; Fretwell 1972), is a mainstay of the theoretical repertoire of behavioral ecology: it deals with the ecologically and behaviorally important problem of the spatial distribution of foraging animals. Its simplicity makes it a frequent starting point for new theoretical developments. Theoreticians have extended and modified the IFD in several ways: (1) allowing unequal competitors (e.g., Rosenzweig 1986; Korona 1989; Sutherland and Parker 1992); (2) incorporating resource dynamics (e.g., Schwinning and Rosenzweig 1990; Lessells 1995), and (3) incorporating assessment rules and perceptual constraints (e.g., Abrahams 1986; Bernstein et al. 1988). Moreover, the IFD lends itself to experimental and empirical study, Tregenza's (1995) review lists 48 empirical studies from 1970 to 1995. Although some disagree about the empirical success of the model (Parker and Sutherland 1986; Kacelnik et al. 1992; Kennedy and Gray 1993; Milinski 1994; Tregenza 1995), many observers are struck with how well the IFD agrees with the data given its simple (and seldom realized) assumptions.

This paper attempts to place the IFD in an explicitly spatial context. The reader may find this a curious goal, since the IFD is unquestionably a spatial model. However, the IFD is not really a model of the distribution of animals *in space*; it is, instead, a model of the distribution of animals *among patches or sites*. The spatial entities in the IFD are a set of well-defined, distinct sites, and the IFD provides no a priori guidance about how these sites should be identified. Most of us would agree that properties of resources (e.g., renewal rate, map position, initial density) and properties of foragers (consumption rates, movement speed, perceptual limitations) will be part of any biological definition of sites. A spatially explicit IFD might formalize this definition. In addition, the IFD assumes distinct hard-edged sites, even though natural resources are often more like smoothly changing resource gradients. Again, this is an issue that a spatially explicit IFD might address.

### The elementary IFD: an implicit spatial model

Consider two possible feeding sites, numbered 1 and 2. In the conventional IFD, we imagine a non-breeding population of mobile animals of size $N$, where $n_1$ is the number of individuals at site 1 and $n_2$ is the number of individuals at site 2 ($n_1+n_2=N$). We characterize each

Communicated by A. Kacelnik

D.W. Stephens (✉) · J.R. Stevens
Department of Ecology, Evolution and Behavior,
University of Minnesota, St. Paul, MN 55108, USA
e-mail: dws@forager.cbs.umn.edu
Tel.: +1-612-6255722, Fax: +1-612-6246777

site by a rate of food arrival, $r_1$ and $r_2$, and we suppose that the $n_i$ individuals in site $i$ compete as coequal exploiters so that each obtains food at rate $\frac{r_i}{n_i}$. We seek an $(n_1, n_2)$ pair such that no individual can benefit from moving to the alternative site. These assumptions suggest an arrangement of individuals such that

$$\frac{r_1}{n_1} \approx \frac{r_2}{n_2}, \quad (1)$$

because if an individual leaves site 1 for site 2, it will necessarily do worse

$$\frac{r_1}{n_1} \approx \frac{r_2}{n_2} > \frac{r_2}{n_2 + 1} \quad (2)$$

Notice that this simplest model relies on exploitation competition: at each site, individuals compete in a scramble to obtain food; the more individuals present, the lower the gains per individual.

## The model

This simple model says virtually nothing about what a site is. To be concrete, imagine that sites are point sources that we can locate at specific map positions. Does the spatial relationship between the two sites matter? Certainly it does. Sites separated by millimeters present a different spatial problem than sites separated by kilometers. We present an IFD model than accounts for the effects of distance by assuming that a forager's gains gradually decrease as its distance from a site increases. The next section gives a verbal and graphical development of our model. The Appendix presents a detailed algebraic development.

### The one-player, optimization model

To begin, consider a single forager exploiting a single point source. The source is at position $s$ and delivers food at constant rate $r$ (i.e., we consider the so-called "continuous input" case). The forager is at position $x$. How does the forager's position affect its benefits? If we follow the traditional IFD, we might require that the forager position itself at the source position ($x$=$s$) to obtain any food. However, this seems too extreme: a forager close to but not precisely at $s$ may do quite well. To say how well, we must consider the variance in delivery positions about the source and the forager's ability to reach food at a distance. We assume that food delivery positions follow a normal distribution, with mean $s$ and variance $\sigma^2$ (Fig. 1); and, that a second Gaussian function describes the forager's ability to reach food delivered at a distance. This reach function peaks at the forager's position $x$, and tapers off according to width parameter $h^2$ that is analogous to the variance of a normal distribution (Fig. 1A). Although $\sigma^2$ and $h^2$ describe the properties of mathematically different types of functions, we may reasonably refer to both as width parameters.

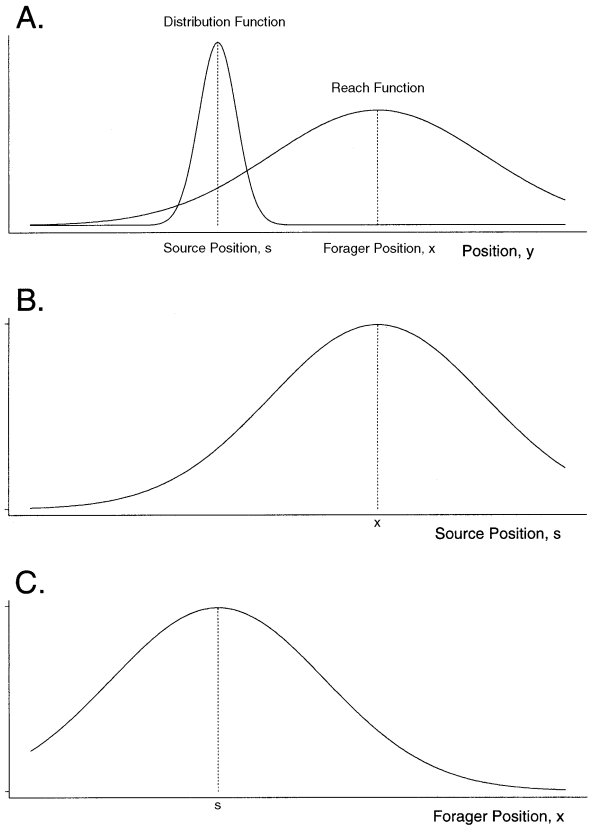


**Fig. 1** **A** A distribution function centered at $s$ with width parameter $\sigma^2$, and reach function centered at $x$ with width parameter $h^2$. **B** The exploitation function [$G(x,s)$] that results from combining the distribution and reach functions as a function of $s$; centered at $x$ with width parameter $\sqrt{\sigma^2+h^2}$. **C** The same exploitation function as a function of $x$; now centered at $s$ with width parameter $\sqrt{\sigma^2+h^2}$

We choose Gaussian functions for several reasons. A Gaussian distribution function is a natural extension of the discrete sites of the IFD: a site is centered at a given mean position with a variance component that gives it fuzzy edges. In addition, this models natural situations where food, released from a central place (e.g., seeds from a flower head, insect larvae from an egg mass), moves by diffusion upon release. Our idea that another Gaussian function describes the forager's ability to reach food at a distance is a plausible first conjecture. Ultimately, we will need empirical guidance to validate or refine this idea.

We want to know how the forager's position ($x$) relative to the source position ($s$) affects the benefits it obtains [say $G(x,s)$]. Formally, we can find this function by integrating the product of the distribution and reach functions (see Appendix). Figure 1B, C shows that we can think of the resulting function in two ways. If we hold the forager's position ($x$) constant and vary the source position ($s$), then we expect a Gaussian function centered at $x$ (Fig. 1B). If, instead, we hold the source position constant and vary the forager's position, we expect the same Gaussian curve, but now centered at $s$ (Fig. 1C). We call this function [$G(x,s)$] the exploitation function, because it shows how the properties of forager

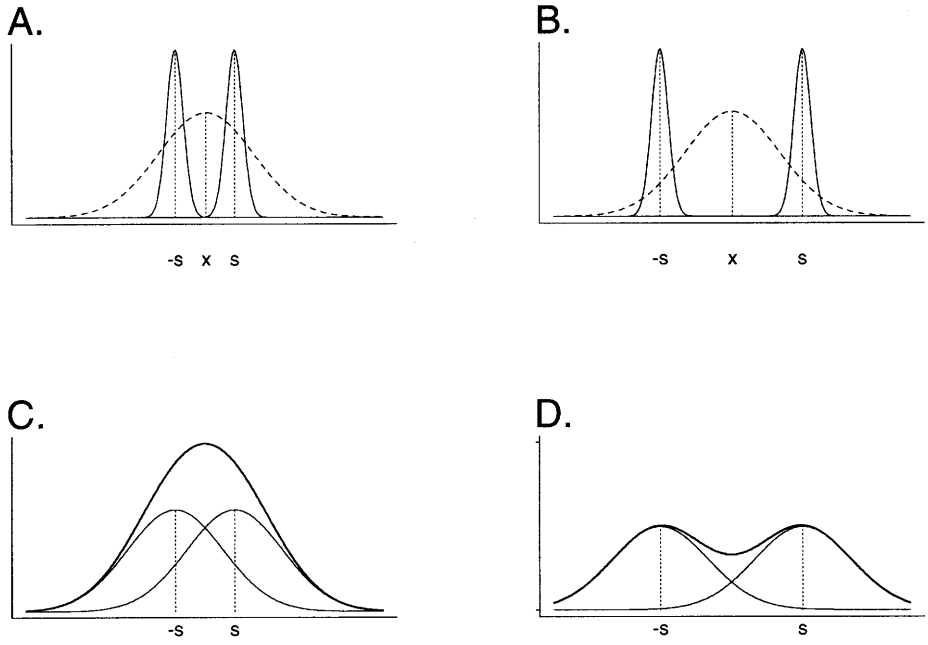


**Fig. 2** Shown in **A** and **B** are two narrow distribution functions as *solid curves*. These distribution functions are centered at $-s$ and $s$. They also show a Gaussian reach function for a forager positioned in the center ($x$=0). **C** and **D** show the corresponding exploitation functions (**C** corresponds to **A** and **D** to **B**). The *heavy curves* in **C** and **D** show the sum of the individual exploitation curves. In **A** and **D**, the sources are close together, and a forager position in the center can exploit both; so the total benefit curve in **C** peaks in the center. In **B** and **D**, the sources are further apart, so a forager positioned in the center exploits both poorly; thus the total benefit curve in **D** has a minimum in the center and two coequal maxima near the source positions

and source combine to determine the consequences of exploitation at distance. Although it is Gaussian in form, the exploitation function is broader than both the distribution and reach functions, having width parameter $\sqrt{\sigma^2+h^2}$. This will be a central parameter in our model, and we call it the exploitation width.

## Two sources

Consider a forager who must choose a position when there are two equivalent sources. The forager faces a trade-off: it can choose a position near one source that maximizes the benefit it extracts from this close source, or it can choose a central position that attempts to use both sources. We expect intuitively that a central position will be best when the two sources are very close together, and that a non-central position that focuses on one source will be best when the sources are widely separated.

### *Notation*

We place these two equivalent sources at positions $-s$ and $s$. That is, we choose a coordinate system that fixes 0 half way between the two sources. This means that $2s$ is the distance between the two sources, and we call it the *source separation*. The parameter $s$, which we call the *source position*, completely determines the source separation ($2s$), and so we may use whichever is most convenient for a particular analysis.

We use the exploitation functions described earlier to evaluate the two-source problem. We suppose that the combined benefits from the two sources are the sum

$$G(x,-s) + G(x,s).$$

Figure 2 shows how we can use this sum-of-benefits formulation to understand the two-source problem. Figure 2A shows two distribution functions as solid curves and a dashed reach function for a forager near the center. Figure 2C shows the exploitation functions [$G(x,-s)$ and $G(x,s)$] that correspond to each source, and, as a heavy line, the total benefits [$G(x,-s)+G(x,s)$]. In this case, we predict that the forager should adopt a central position because the total benefit curve is maximized at $x$=0. Figure 2B, D shows a situation in which the two sources have been moved farther apart. When the sources are widely separated, the central position is a minimum rather than a maximum. This reflects the fact that a central position leaves the forager too far from both sources to extract much benefit from either. When we sum two widely separated exploitation functions we find a pronounced dip in the middle and two coequal maxima near $\pm s$.

This graphical analysis confirms our intuition that the best position is in the middle exploiting both sources when the sources are close together, but near one of the sources when the sources are widely separated. Where does this bifurcation occur? The Appendix shows that foragers should adopt a central position when

$$s < \sqrt{\sigma^2 + h^2}$$

and a non-central strategy otherwise. The reader will recall that $\sqrt{\sigma^2 + h^2}$ is the exploitation width; in words, then, the bifurcation point occurs when the source position equals the exploitation width (cf. Fig. 3A, B). Generally speaking, foragers should be more likely to adopt a central position when the exploitation width is large.

Although it is difficult to find an analytical expression for the optimal positions, the Appendix derives a complete, qualitative characterization of the optima, showing that the optimal positions sweep out a pitchfork-shaped

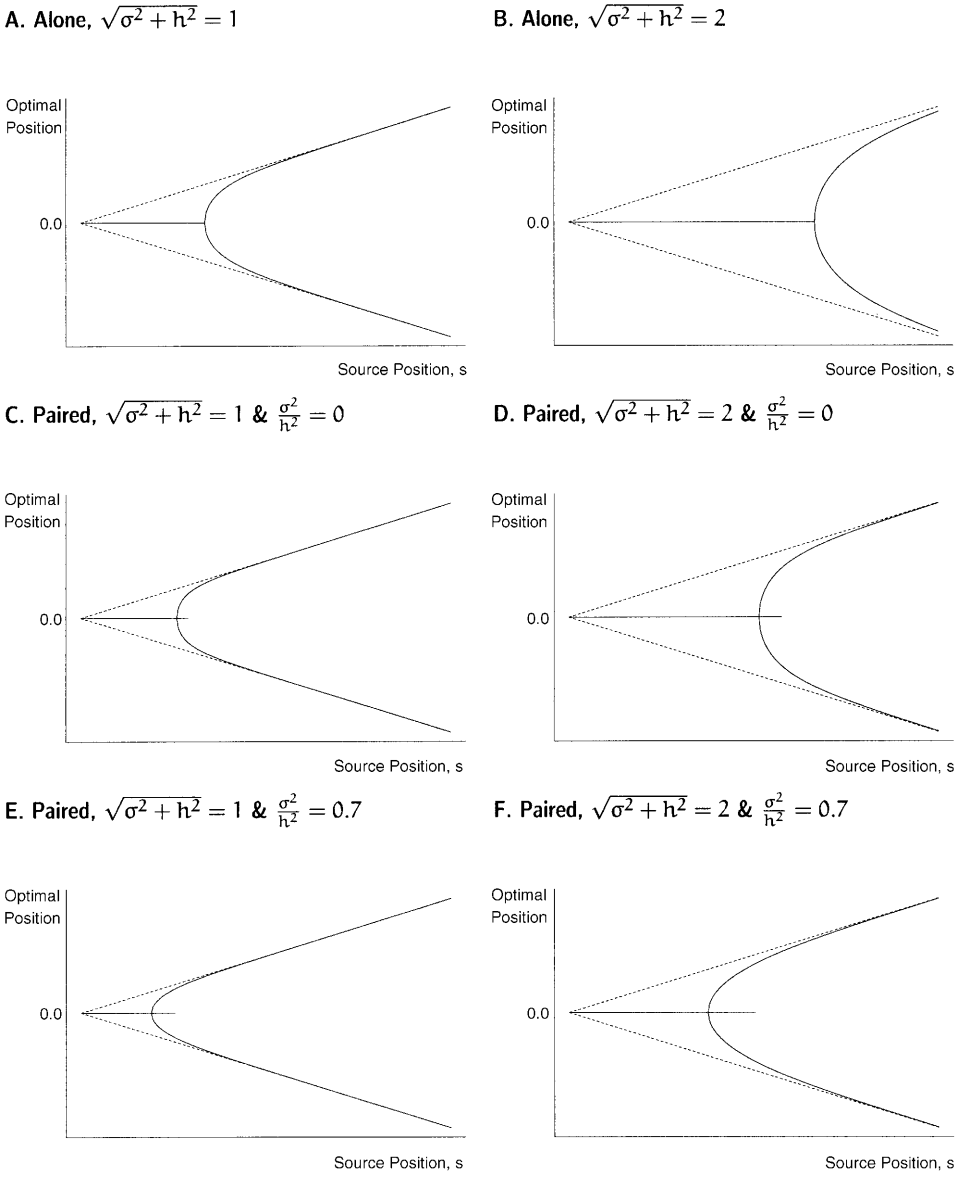


**Fig. 3A–F** Plots of theoretical predictions for various conditions and parameter values. The *solid lines* show predicted positions, the *dashed lines* show the source positions for comparison

pattern as source position ($s$) increases (Fig. 3A, B). For small source separations, the best position is a central one; as source separation increases, there is a qualitative change to two non-central optima. At large source separations, these non-central optima track the source positions ($\pm s$) closely (as one expects).

Even though we cannot find an analytical expression for the optima, we have found a satisfactory approximation (see Appendix for justification):

$$x^* \approx \begin{cases} 0 & s < \text{when } \sqrt{\sigma^2 + h^2} \\ \pm s \tanh\left(\sqrt{3\left(\frac{s^2}{\sigma^2 + h^2}\right)}\right) & \text{otherwise} \end{cases}$$

We used this approximation to plot Fig. 3A, B, and to derive predictions for our experiment.

NE-$x$ models: the two-player game

In this section, we consider a game with two competitors where we solve for the Nash equilibrium (NE) positions ($x$) of two players: hence the name NE-$x$ models. To develop a spatial game, we must know how the presence of a competitor changes the optimality model outlined above. If we have two foragers, one at $x_1$ and another at $x_2$, their reach functions tell us how effectively they exploit food at $y$. It follows that these reach functions should specify the intensity of exploitation competition at $y$. The Appendix shows how we can combine the reach functions of two foragers [say $\pi_1(y,x_1)$ for focal individual 1, and $\pi_2(y,x_2)$ for competing individual 2] into a new *effective* reach function that incorporates information about the forager's reach and about the effects of competition implied by the competitor's reach. The Appendix justifies the use of

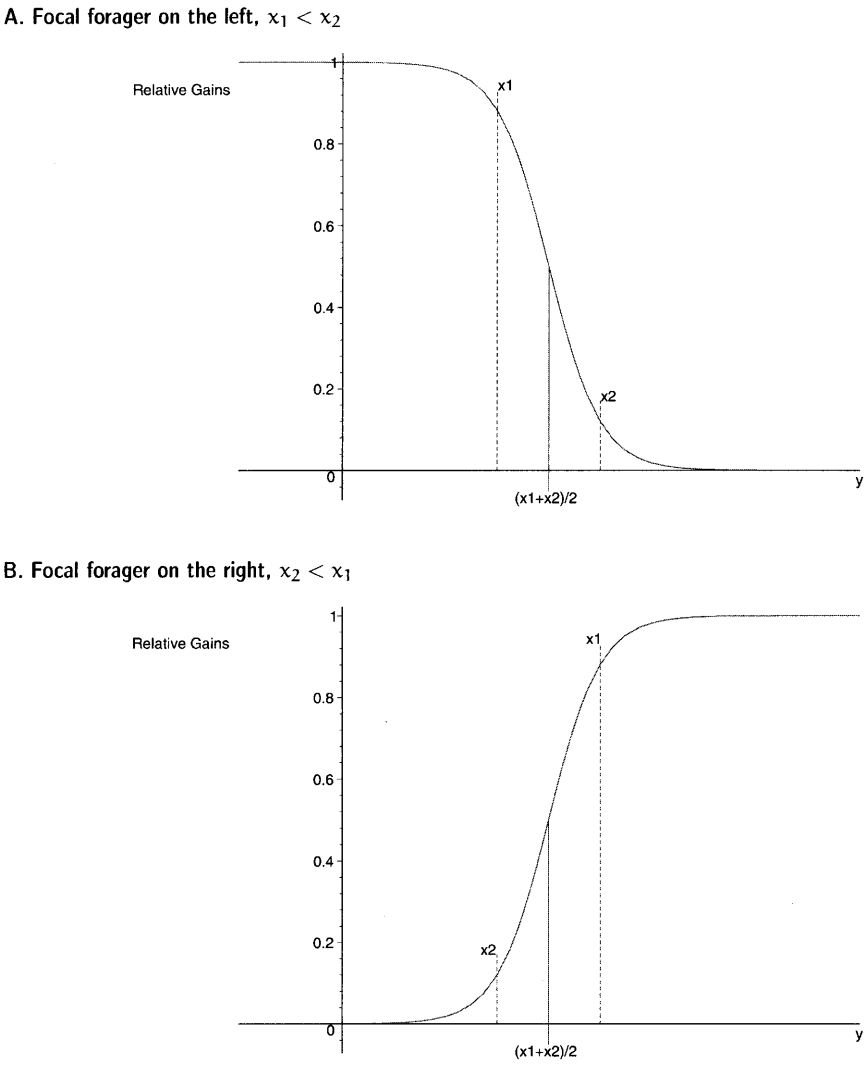


**Fig. 4A, B** Two plots of Eq. A13. This shows how forager 1's relative gains vary with position *y* in two cases. In the *top panel*, forager 1 is to the left of forager 2 ($x_1<x_2$); so on the far left, forager 1 obtains 100% of the gains it would obtain alone, while on the far right it obtains virtually nothing. In the *bottom panel*, forager 1 is on the right ($x_1>x_2$) and we have the mirror image situation with high relative gains on the right, and low relative gains on the left

$$\xi(y,x_1,x_2)=\frac{\pi_1(y,x_1)}{1+\frac{\pi_2(y,x_2)}{\pi_1(y,x_1)}}$$

as a suitable, but approximate, effective reach function. This formulation agrees with the traditional IFD in two important special cases. If at a given position, both foragers have the same capture probability [$\pi_2(y,x_2)=\pi_1(y,x_1)$], then the forager's "normal" probability of capture is halved $\xi(y,x_1,x_2)=\frac{\pi_1(y,x_1)}{2}$, as when two foragers are present at the same site in the traditional IFD. If, on the other hand, the competitor is very far from position *y*, then its probability of capture will be close to zero and the focal forager's reach function is unchanged [$\xi(y,x_1,x_2)\approx\pi_1(y,x_1)$], as when a single forager finds itself alone in the traditional IFD. The term

$$\frac{1}{1+\frac{\pi_2(y,x_2)}{\pi_1(y,x_1)}}$$

represents the effects of competition, since we multiply the reach function by this factor to obtain the effective reach function. This term varies between 0, meaning the competitor dominates at a position *y*, and 1, meaning that there is no effective competition at *y*. This competition factor therefore expresses the forager's gains relative to what it could obtain if alone. Figure 4 shows the behavior of this competition factor for Gaussian reach functions (Eq. A13). The intensity of competition depends on the difference $x_1-x_2$ and the mean position of the foragers, $\frac{x_1+x_2}{2}$. In most situations, the competition factor is a sigmoid function of position *y*. When our focal forager is to the left (Fig. 4A) of the competitor ($x_1<x_2$), then the focal forager's relative gains are near one on the left and near zero on the right, and equal to one-half at the inflection point precisely between the foragers $\left(y=\frac{x_1+x_2}{2}\right)$. When the focal forager is on the right (Fig. 4B), we have the mirror image situation in which competitive ability increases as *y* moves to the right. In the special case in which both foragers occupy the same position, the sigmoid degenerates into a flat line at $\frac{1}{2}$.

The next step is to calculate the total benefits to an individual at $x_1$ with a competitor at $x_2$. Here, we follow the logic of the optimization model except that we use

the effective reach function in place of the ordinary reach function. The Appendix documents the details of these calculations. To find an analytically tractable benefit function, we restrict ourselves to the "point source" case in which $\sigma^2<h^2$ (i.e., the variance about each source is less than the forager's reach). With an expression for total benefit in hand, we calculate NE positions for a pair of foragers. While these calculations are tedious (see Appendix), we can characterize the results easily (Fig. 3). The NE-*x* positions are qualitatively similar to the optimal *x* positions in that both cases show a pitchfork pattern with increasing source separation *s*.

However, there are several important differences. First, in the optimization model, the upper and lower tines of the pitchfork are coequal optima and the forager should be indifferent between them. In the two-player game, we expect a definite pattern, with one forager on the upper branch and another on the lower branch. Second, the handle of the pitchfork represents a pair of NE in the center ($x_1=x_2=0$). In Fig. 3C–F, the pitchfork has a short central tine; this shows situations where there are two NE, one in the center ($x_1=x_2=0$), and a different pair of non-central values ($x_1=-x_2\neq 0$). Finally, in the optimization model, the exploitation width $\left(\sqrt{\sigma^2+h^2}\right)$ completely determines the optima, so any combination of $\sigma^2$ and $h^2$ such that $k=\sqrt{\sigma^2+h^2}$ gives the same result. This is not true in the two-player game. Although the exploitation width is still a key variable, the relative magnitudes of $\sigma^2$ and $h^2$ (specifically the term $\frac{\sigma^2}{h^2}$) are also important. As the quotient $\frac{\sigma^2}{h^2}$ increases, the bifurcation point decreases (compare Fig. 3C, E with Fig. 3D, F). A comparison of the one-player (Fig. 3A, B) and two-player (Fig. 3C–F) plots shows that paired foragers should adopt non-central positions at smaller source separations.

As in the one-player case, we specify the solutions approximately (see Appendix). When

$$s<\sqrt{(\sigma^2+h^2)\left(\frac{3}{4}-\frac{\sigma^2}{4h^2}\right)}\,\text{then}\,(x_1,x_2)=(0,0)$$

is a Nash Equilibrium. When

$$s>\sqrt{(\sigma^2+h^2)\left(\frac{3}{5}-\frac{2\sigma^2}{5h^2}\right)}\,\text{then}$$

$$(x_1,x_2)\approx\left(\pm s\tanh\left(\sqrt{6\left(\frac{s^2}{\sigma^2+h^2}\frac{3}{5}+\frac{2\sigma^2}{5h^2}\right)}\right),\right.$$

$$\left.\mp s\tanh\left(\sqrt{6\left(\frac{s^2}{\sigma^2+h^2}-\frac{3}{5}+\frac{2\sigma^2}{5h^2}\right)}\right)\right) \qquad (3)$$

is a Nash Equilibrium. The Appendix compares this approximation to numerically calculated exact solutions.

### *Model summary*

Imagine an experiment in which one or two foragers must choose positions along the line connecting two point sources. The experimenter systematically varies the distance between the two sources. Our models predict that the relationship between source position and forager position should follow a pitchfork pattern (Fig. 3). In each of these plots there is a critical *s* value at which non-central solutions first arise (i.e., the bifurcation point). The following list summarizes our results in terms of this bifurcation point: (1) the bifurcation point increases with the exploitation width $\left(\sqrt{\sigma^2+h^2}\right)$ in both the one- and two-player cases; (2) the bifurcation point is smaller in the two-player case, so paired foragers should begin to specialize on one of the sources at smaller separations; (3) in the two-player game, the bifurcation point decreases with $\sigma^2$ and increases with $h^2$.

## Methods

We engineered a system in which foragers position themselves along a line, and where we could systematically vary the positions of two point sources. We used this system to perform the experiment described in the previous paragraph.

The subjects were eight wild-caught adult European starlings (*Sturnus vulgaris*), assigned to four pairs (one male/male, one female/female, and two mixed-sex pairs). We conducted the experiments in a 2.7×2.7×2.7 m room illuminated by standard fluorescent lighting and equipped with a white-noise generator to mask extraneous noise. The birds learned to feed from a pair of pellet dispensers mounted on an inclined plane. Collectively we call this the "roof" apparatus (Fig. 5). During feeding sessions, each dispenser delivered, on average, one pellet every 8 s. These delivery schedules were statistically independent. The starlings typically perched on the lip formed at the base of the roof and intercepted pellets as they rolled down the roof. Any pellets that reached the base of the roof fell into a chamber where the birds could not reach them. The idea was to make the bird's "position" along the lip of the roof the key variable in its foraging success, and to prevent a behavioral pattern of hopping back and forth to collect accumulated food.

### Treatments

The two pellet feeders represent the two "point sources" in our models, and our dependent variables are the starling's *x* positions along the lip of the roof. We restrict our attention to the starling's position along the lip, where the starlings spent most of their time (linoleum covered the surface of the roof and starlings seemed reluctant to land on this slippery surface). The four pairs were studied in sequence with each pair experiencing 21 treatments in random order. The 21 treatments were factorial combinations of seven source separation treatments (0, 10, 20, 30, 40, 50, and 60 cm), and three grouping treatments (paired, bird A alone, bird B alone). The experiment ran as a closed economy with birds living in the experimental room 23 h/day (a daily 1-h break for cleaning, weighing, and equipment maintenance). The apparatus delivered food in two 45-min sessions each day: one session from 1015 to 1100 hours and another from 1515 to 1600 hours. We adjusted feeder positions and grouping condition according to a predetermined random schedule 2.75 h before food delivery began in each session. In unpaired treatments, we moved one of the birds to a small, centrally located cage (placed on the floor about 0.5 m in front of the apparatus) so that the focal bird could see its partner, but the partner could not forage. We videotaped the first 30 min of food delivery in each session, and later recorded each starling's *x* position every 20 s within this observation period.

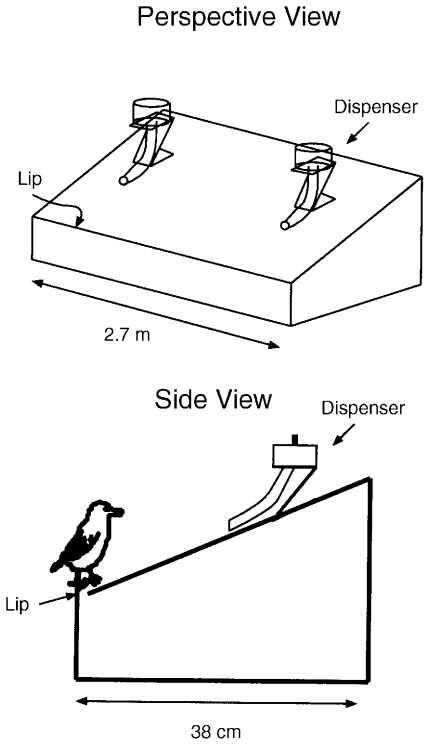


**Fig. 5** Diagram of roof apparatus

Parameter estimation

The exploitation width $\left(\sqrt{\sigma^2 + h^2}\right)$ is a key variable in our model, but we were unable to control it in our experiment. While we could control and measure the relevant properties of our experimental sites (e.g., the source variance, $\sigma^2$), we only have crude ideas about the foragers' reach ($h^2$).

*Source variance*

Preliminary trials, run without any birds present, confirmed that placement of the feeders gave accurate control over the mean position of pellet delivery. We used these data to estimate the standard deviation of delivery position, and found $\sigma$=9.25 cm, which gives $\sigma^2$=85.6 cm$^2$. Visual inspection of the histograms from these preliminary trials supports the view that delivery position is approximately normally distributed.

*Forager's reach*

One would like to measure the probability of successful consumption when a food item is delivered at a range of distances (i.e., to directly measure the reach function). Unfortunately, we were unable to make these observations with our apparatus. Informal observations suggested that starlings could reach items between 15 and 25 cm away, crudely 1–1.5 body lengths; while they did occasionally "capture" items at greater distances, these successes were relatively rare. If we take $h \approx 20$ cm, then $h^2 \approx 400$ cm$^2$, and $\sqrt{\sigma^2 + h^2} \approx 22$ cm. Similarly, we estimate $\frac{\sigma^2}{h^2}$ to be near 0.2.

Statistical details

Finding statistical estimates of the pitchfork is not straightforward. Suppose that an individual chooses the upper branch of the pitchfork half the time, and the lower branch half the time. This individual's mean position would be zero, a value that does not estimate the branches of the pitchfork in any meaningful way. This suggests that we might consider the absolute value or square of position, effectively folding the lower and upper branches of the pitchfork together to estimate a single value. This folding, however, makes it difficult to evaluate the "handle" of the pitchfork where central positions ($x$=0) are predicted [even if $E(x)$=0, both $E(x^2)$ and $E(|x|)$ will exceed zero, because the error variance will be "folded" onto the positive side of the plane along with any real position effect]. To overcome these problems, we adopted a statistical model that assumed positions $X$ were random variables drawn with probability $p$ from a normal distribution with mean $-k$ and variance $v^2$, and with probability $1-p$ from another normal with mean $k$ and variance $v^2$. From these assumptions, we were able to calculate the distribution of the absolute value of $X$ which depends only on $k$ and $v$ (i.e., $p$ does not affect the distribution of the absolute value). Using the analytically derived absolute value distribution, we calculated maximum-likelihood estimates of $k$ and $v$ for each individual in each separation and grouping treatment. In addition, we extended this technique to test for bimodalities using likelihood ratios. To do this, we calculated the maximum-likelihood estimate of $k$ and $v^2$ (assuming underlying bimodality), and another maximum-likelihood estimate assuming a unimodal distribution by setting $k$=0 and fitting only $v^2$. Next, we used the values of the associated likelihood functions ($\lambda$s) to calculate a likelihood ratio statistic. For a large sample size, the statistic $\Lambda = -2\log\left(\frac{\lambda_{\{0,v^2\}}}{\lambda_{\{k,v^2\}}}\right)$ (where the $\lambda$ indicate the likelihood estimates) is $\chi^2$ distributed with 1 *df* (Mood et al. 1963).

## Results

We designed this experiment to test the idea that positions follow a pitchfork pattern, and to test whether the pitchfork is generally more "spread" in pairs, as our models predict (Fig. 3). Fig. 6 shows histograms of the raw position data lumped for all pairs and subjects. One can see that the pattern is generally as expected, with the distributions moving from unimodal to bimodal as source separation increases. These effects also appear to be more pronounced when the birds are paired, as the model predicts. Strictly speaking, however, we should only expect two equal-frequency modes in the paired data; an isolated individual following our model might produce either a unimodal or bimodal pattern.

Fig. 7 shows the estimated $k$ values and two sets of pitchfork predictions, one (solid curve) that seems to give the best fit to the data $\left(\sqrt{\sigma^2 + h^2} = 13 \text{ cm}\right)$ (fitted by eye), and another (dashed curve) based on our crude estimate of exploitation width $\left(\sqrt{\sigma^2 + h^2} = 22 \text{ cm}\right)$. At small source separations (0, 10, and 20 cm), the median $k$ estimates are very near zero as predicted. ANOVA (Table 1) shows significant ($P$<0.05) effects of pair (i.e., pair identity), source separation, and two significant interaction effects but no effect of grouping (i.e., paired or alone). This $F$-test is based on a small error *df*, and lacks power. We can construct a more powerful test by pooling, if we assume that there is no separation by grouping interaction [$F_{3,4}$=2.67, $P(F \geq 2.67)$=0.182]. An $F$-test based on such a pooled error estimate does show a significant grouping effect [$F_{1,7}$=8.27, $P(F \geq 8.27)$=0.024].

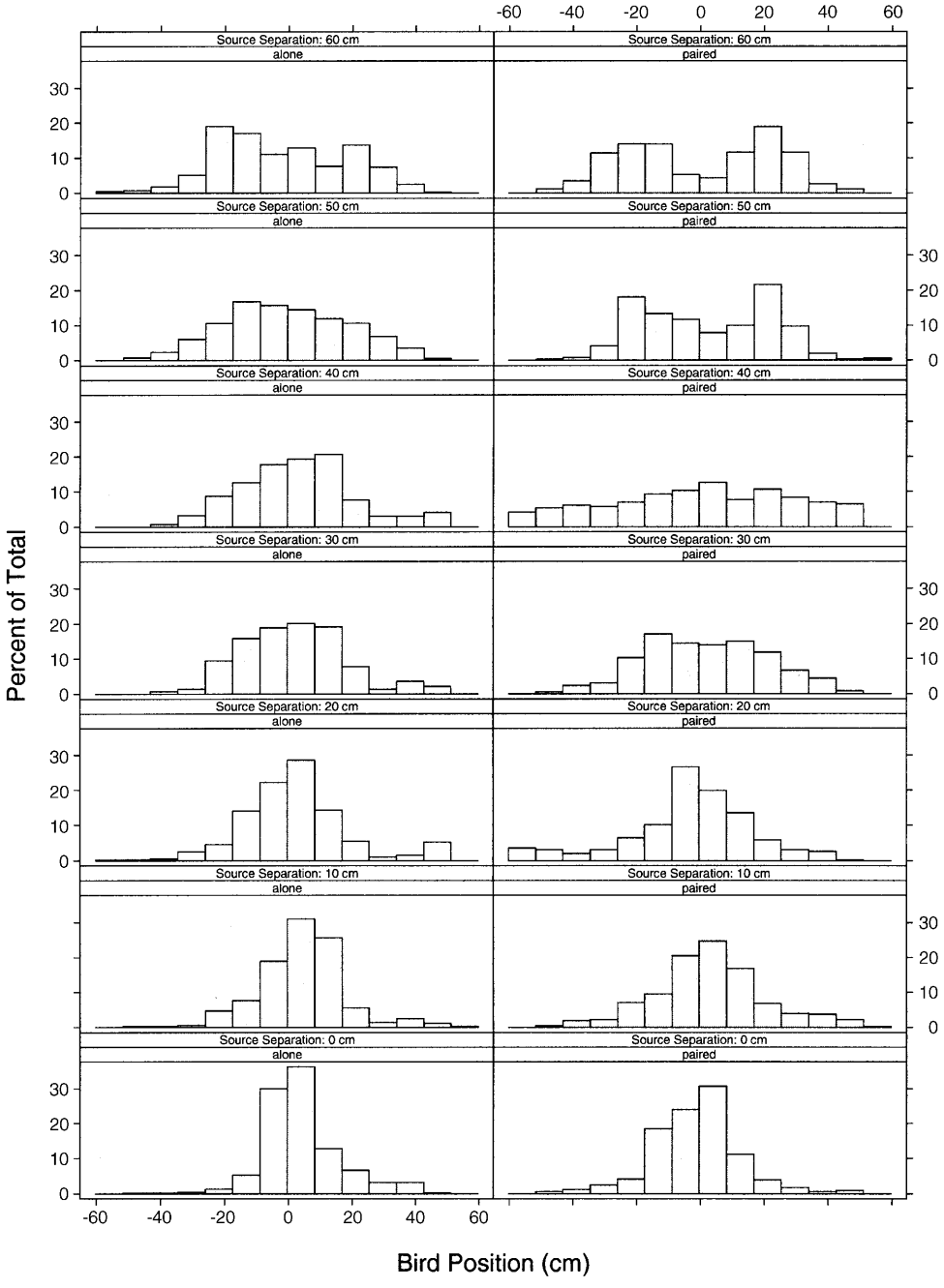


**Fig. 6** Histograms of raw position data. The *left column* shows results for the "alone" treatment, and the *right column* show results for the "paired" treatment. The *rows* show increasing amounts of source separation with 0 separation in the *bottom row* and 60 cm separation in *top row*

**Table 1** Analysis of variance table. Dependent measure is the maximum-likelihood estimate of $k$ as described in the text. $F$-tests are based on expected mean squares as specified in Myers and Well (1995)

| | Source of variation | *df* | Sum of squares | Mean square | *F* | *P*(*F*) |
|---|---|---|---|---|---|---|
| (1) | Pair | 3 | 14.2 | 4.74 | 9.99 | 0.025* |
| (2) | Subjects within pair | 4 | 1.9 | 0.475 | | |
| (3) | Source separation | 6 | 153 | 25.4 | 9.61 | 0.0000832* |
| (4) | Source separation×pair | 18 | 47.7 | 2.65 | 2.08 | 0.047* |
| (5) | Source separation×(subjects within pair) | 24 | 30.5 | 1.27 | | |
| (6) | Grouping | 1 | 14.6 | 14.6 | 5.3 | 0.105 |
| (7) | Grouping×pair | 3 | 8.26 | 2.75 | 2.69 | 0.182 |
| (8) | Grouping×(subjects within pair) | 4 | 4.1 | 1.02 | | |
| (9) | Grouping×source separation | 6 | 22.1 | 3.68 | 0.98 | 0.472 |
| (10) | Grouping×source separation×pair | 15 | 56.3 | 3.75 | 2.64 | 0.022* |
| (11) | Grouping×source separation×(subjects within pair) | 20 | 28.4 | 1.42 | | |

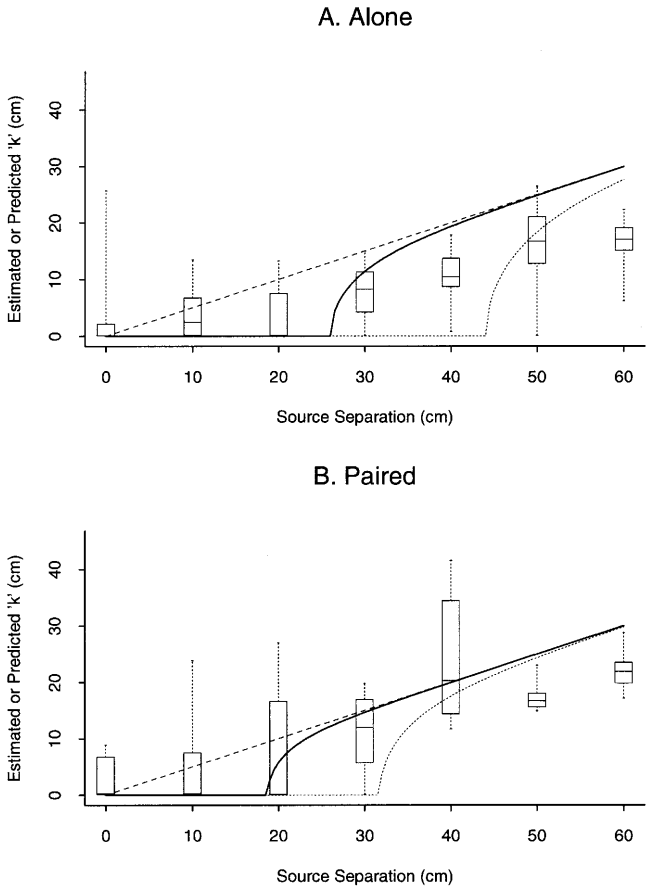


**Fig. 7** Maximum-likelihood estimates of the alone (**A**) and paired (**B**) data. Box plots summarize the data for each separation level (see Cleveland 1993). Each box shows the median (*horizontal line* within the box), 25th and 75th percentile points (*lower* and *upper limits* of the box, respectively, and the extreme values (*whiskers*). The *heavy curve* shows predictions for $\sqrt{\sigma^2 + h^2} = 13$ cm, a value chosen because it gives a good fit to the data, as judged by eye. The *dashed curves* show predictions for our a priori estimate value of $\sqrt{\sigma^2 + h^2} = 22$ cm. In **B** the assumption is that $\frac{\sigma^2}{h^2} = 0.2$, as estimated from our data. The *dashed line* shows the position of the source

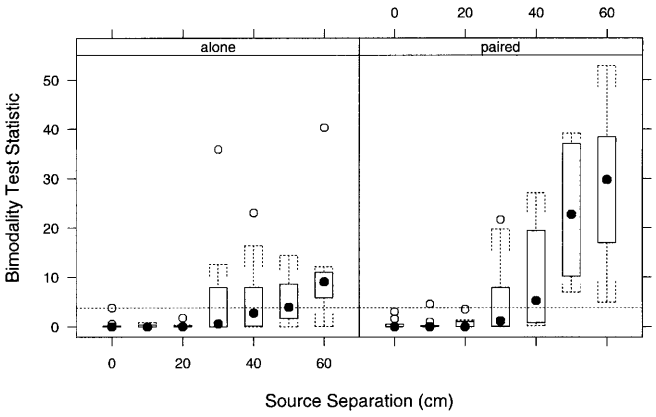


**Fig. 8** Values of log-likelihood test statistic $\Lambda$ testing the hypothesis that $k$=0 (i.e., the position distribution is unimodal). The *dashed line* shows the critical value. We reject the hypothesis of unimodality if $\Lambda > \chi^2_{0.95}(1) = 3.84$. Note that $\Lambda$ was calculated for individual birds, so the evidence for bimodality in pairs should not, in principle, be enhanced because we are examining a mixture of the positions of two individuals

In addition, Fig. 8 shows calculated bimodality test statistics (see Methods) for each bird in each treatment combination. This figure strengthens the case for a paired-alone difference, by showing that evidence for bimodality is stronger in the paired treatment (recall that these measures are assessed per individual, so bimodality is not a necessary consequence of the paired condition).

The data support our prediction that animals should occupy the "center" until the distance between resources exceeds some threshold (Figs. 7, 8). However, our crude estimate of exploitation width $\left(\sqrt{\sigma^2 + h^2} \approx 22 \text{ cm}\right)$ seems too large, since the data suggest a value near 13 cm. Although this effect was not strong, the starlings tended to be further from the center in the "paired condition." The clearest contradiction occurs at larger resource separations. Although the birds showed a steady movement outward as source separation increased, they were closer to the center than expected at large resource separations (Fig. 7). This deviation from our predictions holds in both the individual and paired conditions, although it is most striking in the alone condition.

## Discussion

In most of the spatial models of behavioral ecology, the spatial entities – patches, sites, habitats – are discrete and hard-edged (see Arditi and Dacorogna 1988, for a noteworthy exception). Our model explores an elementary approach to softening these edges, which emphasizes the costs and benefits experienced by individuals. Taking the simplest IFD (two point sources, continuous input, two players) as our starting point, we have asked: how does the distance between sources affect an animal's position? This simple question raises issues of general significance: What is the zone of "exploitable" space around a forager like? How does distance affect the intensity of competition? While our answers to these questions must be seen as preliminary, the questions themselves are basic to any complete, spatially explicit foraging theory.

### The model and the data

For two foragers and two equivalent sources, the conventional, distinct-sites IFD predicts one forager at each site. Although the IFD per se makes no prediction about the one-player situation, a single forager following the intake-maximizing logic of the IFD should be indifferent. In both cases, the distinct-site logic of the IFD sug-

gests that foragers should position themselves at one source and ignore the other regardless of source separation. An animal adopting this source-tracking tactic should choose an average position that is the same as the source position, and it should not bias its position to one side or the other. The data show, however, that starlings were biased toward positions *between* the two sources. On average, the birds were 4.05 cm (95% confidence limits: 2.37–5.74 cm) from the source, and up to 10 cm from the closest source when source separation was large. So, our results do not support a source-tracking model.

This evidence against source-tracking also challenges our models, because they predict source-tracking at large source separations. We offer two possible explanations. First, social cohesion may create a bias toward central positions, (recall that a non-foraging partner is present, in a central cage, during the "alone" treatment). However, the deviation toward the central position was strongest in the alone treatment, which is more consistent with competition than social cohesion, since the partner is on average closer in the alone treatment. Second, the Gaussian functions used in our models may over-emphasize proximity. Functions that are more "broad-shouldered" than a Gaussian might explain our results. If starlings can do nearly as well at 10 cm from the source as they can from 0 cm, then this tactic may put them 10 cm closer to the alternative source without sacrificing gains from the closer "primary" source.

We have imagined Gaussian reach and distribution functions that, we feel, are reasonable guides to our intuition. There are, however, many other possibilities. It is difficult to generalize about alternative distribution functions because almost anything is possible – resources may be concentrated at a single point, spread uniformly throughout a given space, or have many peaks of abundance. While one can apply the principles outlined here in even the most complex situations, we do not expect the simple predictions of our model to apply in all situations. As mentioned earlier, we expect the motor and sensory abilities of the forager to determine the reach function. The reach function for a laterally oriented electrolocating fish will certainly differ from a starling's. Incorporating these differences is an important challenge for our approach.

## Extensions and alternatives

While our models have focused on simple, experimentally tractable situations (two players, two sources, and one spatial dimension), the principles at work are general. It is not difficult to calculate a focal individual's gains in a many-player, continuous-gradient version of our model. However, it is difficult to find the many-player equilibrium using this calculation. In most cases, one will have to find this solution numerically. This is typical of spatially explicit models, and it is one reason why multiple approaches are so important (see Tilman et al. 1997).

### *Other approaches*

Sasaki (1997) presents a model that complements ours. Sasaki's basic model is a modified Lotka-Volterra competition model with diffusive movement, in which a probability distribution function specifies the spatial distribution of a population of mobile animals. In addition, a Gaussian function of competitor proximity determines the intensity of competition. In contrast with our model, Sasaki assumes that a forager can only exploit resources at its position, (in our terminology, the zero-reach case). Sasaki shows that individuals should be clumped even in a uniform resource gradient. Sasaki's approach complements ours, because it models an important many-player situation. Another family of models that addresses the spatial consequences of feeding decisions has focused on the vertical migration and distribution of zooplankton (e.g., Iwasa 1982; Gabriel and Thomas 1988; Giske et al. 1997). Of these, the paper by Giske et al. (1997) makes the most explicit connection to the IFD.

### *Rule-based models.*

Our model [like those of Sasaki (1997) and Giske et al. (1997)] focuses on the economics of position. An alternative, and only partially explored, approach is to consider the economics of movement rules and then to deduce the consequences of these rules for spatial distributions. For example, a population in which each individual follows a gradient-climbing rule will reach a predictable spatial distribution, and given sufficient information about the spatial distribution of resources, we should be able to calculate this. The mathematical advantage of a rule-based approach is that all individuals can use the same rules, even though they cannot adopt the same positions, so a rule-based approach may generalize to large numbers of players more easily (see Bernstein et al. 1988, 1991 for an example).

## Spatial issues in the IFD

Theoreticians have modified the IFD in many ways (see Tregenza 1995 for review). In the next few paragraphs, we discuss how our approach complements three important themes in IFD modeling.

### *Interference models*

Since the publication of Sutherland's (1983) seminal paper, it has become conventional to distinguish between continuous-input models (as developed here and by Fretwell and Lucas 1970) and interference models (as developed by Sutherland). The interference models are commonly applied to field situations in which prey is very abundant and depletion relatively unimportant. In addition, it is widely reported (Parker and Sutherland

1986; Kacelnik et al. 1992) that these interference models do not fit the data as well as the continuous models. Although we have restricted ourselves to exploitation competition, spatially explicit techniques may provide a powerful way to model interference competition.

### *Competitive asymmetries*

Many students of the IFD have emphasized competitive asymmetries (Parker and Sutherland 1986; Rosenzweig 1986; Sutherland and Parker 1992). Each of these models must somehow solve the problem of mathematically representing a range of competitive abilities. The models developed by Parker and Sutherland, for example, assume that each individual has an intrinsic competitive "weight." These weights are rather ad hoc measures, and one is bound to wonder where they might come from. Thinking spatially can provide a new way to think about competitive asymmetries. For example, one can imagine a situation where individuals have measurably different reach functions that determine their competitive abilities.

### *Resource dynamics*

A third area where an explicitly spatial perspective might prove rewarding is in models allowing more complex resource dynamics, e.g., accumulation and depletion. When accumulation and depletion are allowed, stable patterns of movement between sites can be an important part of the solution (see for example Schwinning and Rosenzweig 1990). Clearly, the costs and effectiveness of movement between sites depend on the explicit spatial arrangement of sites.

## The spatial scale of behavioral ecology

Many questions in behavioral ecology are fundamentally spatial questions, and behavioral ecology has a rich tradition of spatial modeling. Most of these models view the world as a patchwork of distinct recognizable sites. Yet, we have no theory to guide our attempts to superimpose a patchwork on a natural world of fuzzy boundaries. We have considered the spatial scale of patchiness via theory and experiment. Our approach offers a way to formalize these fuzzy boundaries, and our preliminary experiment shows how these problems can be studied.

## Appendix

### Optimal position for an individual

Imagine a single forager at position $x$ along a line. We want to know how the forager's position affects the benefits it receives. Consider the probability that a particle of food will arrive at position $y$. If food arrival positions follow a normal distribution, then the probability that a source at $s$ will deliver a particle of food in the interval $[y,y+dy]$ is:

$$\Pr(\text{food at } y) = f(y)dy = \frac{e^{\frac{(y-s)^2}{2\sigma^2}}}{\sigma\sqrt{2\pi}}dy$$

where $\sigma^2$ is the variance in food delivery position about central position $s$.

We consider, in addition, another Gaussian function that we call the *reach function*. This reach function determines the probability that a forager will capture an item delivered at $y$ when it is positioned at $x$.

$$\Pr(\text{capture food} \mid \text{food at } y \,\&\, \text{forager at } x) = \pi(y) = p_0 e^{-\frac{(y-x)^2}{2h^2}}$$

For example, the forager captures items with probability $p_0$ if they arrive at its position ($y$=$x$), but the probability of capture decreases as the distance between $x$ and $y$ increases. The parameter $h^2$ determines the width of the forager's reach; if $h^2$ is small, the probability of capture falls quickly with distance, but it decreases more slowly if $h^2$ is large.

The total probability of capturing a particle at $y$ is the product of the reach and distribution functions:

$$p_0 e^{-\frac{(y-x)^2}{2h^2}} \frac{e^{-\frac{(y-s)^2}{2\sigma^2}}}{\sigma\sqrt{2\pi}}dy$$

To calculate the overall probability of capturing an item dispensed by the source at $s$, we integrate over all possible delivery positions:

$$\int_{-\infty}^{\infty} p_0 e^{-\frac{(y-x)^2}{2h^2}} \frac{e^{-\frac{(y-s)^2}{2\sigma^2}}}{\sigma\sqrt{2\pi}}dy = \frac{p_0 h}{\sqrt{h^2+\sigma^2}} e^{-\frac{(x-s)^2}{2(\sigma^2+h^2)}} \quad \text{(A1)}$$

Taken together, the reach and spatial distributions behave like a single Gaussian function with width parameter $\sigma^2$+$h^2$. We call this the exploitation function, and we call $\left(\sqrt{\sigma^2+h^2}\right)$ the exploitation width (Fig. 1).

*Two sources.* Next, we suppose that there are two point sources. We position one source at $-s$ and the other at $s$, so that position zero is the center. Now suppose that the source at $-s$ dispenses food at rate $r_1$ and the source at $s$ dispenses food at rate $r_2$. This gives a total benefit of

$$G(x) = \frac{p_0 h}{\sqrt{h^2+\sigma^2}}\left(r_1 e^{\frac{(x+s)^2}{2(\sigma^2+h^2)}} + r_2 e^{\frac{(x-s)^2}{2(\sigma^2+h^2)}}\right) \quad \text{(A2)}$$

*Scaling.* Now, it is natural to think in terms of the exploitation width, $\sqrt{\sigma^2+h^2}$, which represents the width of a zone of exploitation about a point source. Consider the rescaled variables:

$$\hat{x} = \frac{x}{\sqrt{\sigma^2+h^2}},$$

$$\Delta = \frac{s}{\sqrt{\sigma^2+h^2}}, \text{ and}$$

$$g = \frac{\sigma^2}{h^2},$$

with these substitutions, Eq. A2 becomes

$$\frac{p_o}{\sqrt{1+g}}\left(r_1 e^{-\frac{(\hat{x}+\Delta)^2}{2}} + r_2 e^{-\frac{(\hat{x}-\Delta)^2}{2}}\right) \quad \text{(A3)}$$

where we can think of $2\Delta$ as the effective separation of the sources, since it measures the separation of sources in terms of the forager's zone of exploitation. In addition, it is useful to define $p = \frac{\hat{x}}{\Lambda}$, so that $p$ gives the forager's position as a directed proportion: $p$=0 means that the forager is in the center, $p$=–1 means that the forager is at the left source, $p$=1 means at the right, and so on. This gives

$$\frac{p_0}{\sqrt{1+g^2}}\left(r_1 e^{-\Delta^2\frac{(p+1)^2}{2}} + r_2 e^{-\Delta^2\frac{(p-1)}{2}}\right) \quad \text{(A4)}$$

*Optimization*

In choosing $p$ to maximize total benefits (i.e., Eq. A4) we can neglect the common factor $\frac{p_0}{\sqrt{1+g^2}}$, so we maximize

$$r_1 e^{-\Delta^2\frac{(p+1)^2}{2}} + r_2 e^{-\Delta^2\frac{(p-1)^2}{2}}$$

Differentiating with respect to $p$ gives

$$r_1\left[-\Delta^2(p+1)e^{-\Delta^2\frac{(p+1)^2}{2}}\right] + r_2\left[-\Delta^2(p-1)e^{-\Delta^2\frac{(p+1)^2}{2}}\right]$$

factoring

$$-\Delta^2 e^{-\frac{\Delta^2}{2}(p^2+1)}\left[r_1(1+p)e^{-\Delta^2 p} - r_2(1-p)e^{\Delta^2 p}\right]$$

Focusing, now, on the term in square brackets

$$\begin{aligned} 0 &= r_1(1+p)e^{-\Delta^2 p} - r_2(1-p)e^{\Delta^2 p} \\ r_1(1+p)e^{-\Delta^2 p} &= r_2(1-p)e^{\Delta^2 p} \\ \frac{1+p}{1-p} &= \frac{r_1}{r_2}e^{2\Delta^2 p} \end{aligned}$$

taking logarithms of both sides

$$\ln\left(\frac{1+p}{1-p}\right) = 2\Delta^2 p + \ln\left(\frac{r_2}{r^1}\right) \qquad \text{(A5)}$$

While this expression only gives the critical $\left(\frac{dG}{dp}=0\right)$ $p$ values implicitly, it lends itself to a graphical analysis that shows the qualitative properties of the solution. The left-hand side of Eq. A5 is a curve that resembles a vertically stretched plumber's trap (Fig. 9), and the right-hand side is a line with slope $2\Delta^2$ and intercept $\ln\left(\frac{r_2}{r_1}\right)$ [in Fig. 9 $r_1$=$r_2$ so $\ln\left(\frac{r_2}{r_1}\right)=0$]. As the separation between sources ($\Delta$) increases, the line on the right-hand side of Eq. A5 becomes steeper. When the line is shallow, it crosses the curve only at zero, but when it is steeper, it crosses the curve at three points, say $-\hat{p}$, 0, and $\hat{p}$ is some non-zero value). Differentiation of both sides of Eq. A5 shows that the transition from one to three solutions occurs when $\Delta^2$=1. Moreover, we can show that the solution $p$=0 is maximum when $\Delta^2$<1 and a minimum when $\Delta^2$>1; similarly, the pairs of non-zero solutions are always maxima when they occur (i.e., when $\Delta^2$>1). Putting these elements together shows that the graph of optimal position ($p$) versus source separation ($\Delta$) traces out a pitchfork shape, with a single maximum at zero when $\Delta$<1 and two coequal maxima that are symmetric around 0 when $\Delta$>1.

*Approximation*

Although we are unable to solve Eq. A5 for $p$ explicitly, we can find an approximate solution. We recognize that $\ln\left(\frac{1+p}{1-p}\right)$=$2\tanh^{-1}(p)$, substituting into Eq. A5 and rearranging we have

$$\frac{\tanh^{-1}(p)}{p} = \Delta^2 \qquad \text{(A6)}$$

which isolates $p$ on the left-hand side. Next we expand the left-hand side in series, and perform a series reversion (using the computer algebra software Maple) to find

$$p = \sqrt{3(\Delta^2-1)}\,\frac{9}{10}\sqrt{3}\left(\sqrt{\Delta^2-1}\right)^3 + 0\left[\sqrt{\Delta^2-1}^5\right] \qquad \text{(A7)}$$

Now, Eq. A6 suggests something like

$$p = \pm\tanh\left[f(\Delta)\right] \qquad \text{(A8)}$$

where $f(\Delta)$ is an unknown function of $\Delta$. If we choose $f(\Delta) = \sqrt{3(\Delta^2-1)}$, then the first term of a series expansion of Eq. A8 agrees with the first term of Eq. A7. This logic gives the approximate solution

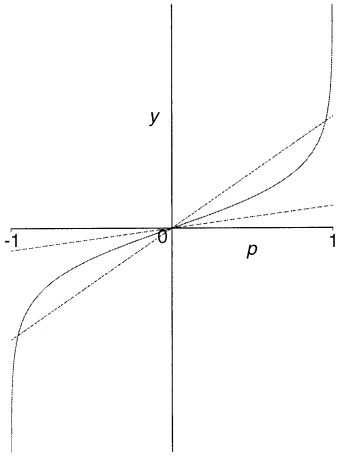


**Fig. 9** Graphical solution of Eq. A5. The *solid curve* is $\ln\left(\frac{1+p}{1-p}\right)$, that is, the left-hand side of Eq. A5. The *dashed line* shows the $2\Delta^2 p$ for $\Delta^2$<1; here the line intersects the curve only once. The *finely dashed line* shows $2\Delta^2 p$ for $\Delta^2$>1; here the line intersects the curve in three places. Generally speaking, as $\Delta$ increases, "the line" rotates counterclockwise about (0,0); as it rotates, there is transition from a single intersection at zero to three intersections

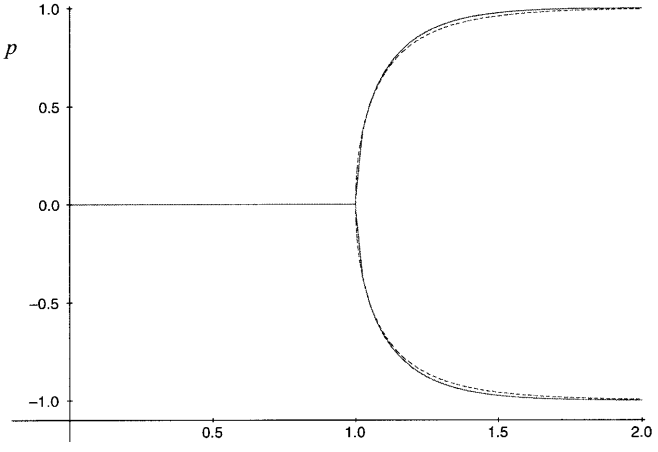


**Fig. 10** *Solid curves* show an exact numerically calculated plot of optimal position $p$ vs source separation $\Delta$. The *dashed curves* show the approximation given by Eq. A9

$$p^* = \begin{cases} 0 & \Delta \le 1 \\ \pm\tanh\left(\sqrt{3(\Delta^2-1)}\right) & \Delta > 1 \end{cases} \qquad \text{(A9)}$$

Figure 10 superimposes this approximation with an exact numerical solution, and shows that there is very good agreement between them.

The two-player game

*Competition in space*

Consider a food particle arriving at position $y$ along our line. Suppose that if feeding alone forager 1 obtains this item with probability $\pi_1$ as specified by its reach function; similarly, if alone, forager 2 obtains this item with probability $\pi_2$. Now, the probability that both will fail to capture the item is $(1–\pi_1)(1–\pi_2)$, so the probability that the item is captured by either forager 1 or forager 2 is

$$1 - (1-\pi_1)(1-\pi_2) = \pi_1 + \pi_2 - \pi_1\pi_2 \qquad \text{(A10)}$$

Now, we would like to know how frequently forager 1 captures the item, given that the item is captured. An application of Bayes' theorem gives:

$$\Pr(1 \text{ captures} \mid \text{Someone captures}) = \frac{\pi_1}{\pi_1+\pi_2} \tag{A11}$$

Combining Eq. A10 and Eq. A11 we have

$$\frac{\pi_1}{\pi_1+\pi_2}(\pi_1+\pi_2-\pi_1\pi_2)$$

which we rewrite as

$$\frac{\pi_1}{\pi_1+\pi_2}+\frac{\pi_1\pi_2(1-\pi_1)}{\pi_1+\pi_2}$$

The term $\frac{\pi_1\pi_2(1-\pi_1)}{\pi_1+\pi_2}$ has the product of three probabilities in its numerator, and it is likely to be small. We, therefore, neglect it and take

$$\frac{\pi_1}{1+\frac{\pi_2}{\pi_1}}$$

as a modified reach function that incorporates competitive effects. This formulation agrees with the conventional IFD in two important cases: if the competitor has no chance of obtaining food ($\pi_2$=0), the focal individual's gains are unchanged; if the competitor has the same probability of obtaining food ($\pi_1$=$\pi_2$), then the focal individual's gains are cut in half.

The reach and distribution functions developed in the previous section can be used to calculate $\pi_1$ and $\pi_2$. Consider food delivery at an arbitrary position $y$ from a source at $s$, when the focal individual is at $x_1$ and a competitor is at $x_2$:

$$\frac{\pi_1(y)f(y)dy}{1+\frac{\pi_2(y)}{\pi_1(y)}}=\frac{p_0 e^{-\frac{(y-x_1)^2}{2h^2}}\frac{e^{-\frac{(y-s)^2}{2\sigma^2}}}{\sigma\sqrt{2\pi}}dy}{1+\frac{e^{-\frac{(y-x_2)^2}{2h^2}}}{e^{-\frac{(y-x_1)^2}{2h^2}}}}$$

where we assumed that the two foragers are equivalent (same $h$ and $p_0$) except for their positions. We can rearrange the quotient in the denominator to make this

$$\frac{p_0}{\sigma\sqrt{2\pi}}\frac{e^{-\frac{(y-x_1)^2}{2h^2}}e^{-\frac{(y-s)^2}{2\sigma^2}}dy}{1+e^{\left(\frac{x_1-x_2}{h^2}\right)\left(\frac{x_1+x_2}{2}-y\right)}} \tag{A12}$$

where the factor

$$\frac{1}{1+e^{\left(\frac{x_1-x_2}{h^2}\right)\left(\frac{x_1+x_2}{2}-y\right)}} \tag{A13}$$

represents the intensity of competition at position $y$. The text gives an intuitive explanation of this term (Fig. 4).

Now Eq. A12 gives the benefits that individual 1 obtains at position $y$ given a source at $s$ and an equivalent competitor at $x_2$. To find the benefits from all possible $y$ positions, we want to integrate

$$\int_{-\infty}^{\infty}\frac{p_0}{\sigma\sqrt{2\pi}}\frac{e^{-\frac{(y-x_1)^2}{2h^2}}e^{-\frac{(y-s)^2}{2\sigma^2}}dy}{1+e^{\left(\frac{x_1-x_2}{h^2}\right)\left(\frac{x_1+x_2}{2}-y\right)}}$$

The problem here is that we cannot integrate this analytically. We can, however, find an approximation using Laplace's method (Nayfeh 1981). Applying this technique we find that

$$\int_{-\infty}^{\infty}\frac{p_0}{\sigma\sqrt{2\pi}}\frac{e^{-\frac{(y-x_1)^2}{2h^2}}e^{-\frac{(y-s)^2}{2\sigma^2}}dy}{1+e^{\left(\frac{x_1-x_2}{h^2}\right)\left(\frac{x_1+x_2}{2}-y\right)}}\approx\frac{\frac{p_0 h}{\sqrt{h^2+\sigma^2}}e^{-\frac{(x_1-s)^2}{2(\sigma^2+h^2)}}}{1+e^{\left(\frac{x_1-x_2}{h^2}\right)\left(\frac{x_1+x_2}{2}-\frac{\sigma^2x_1+sh^2}{\sigma^2+h^2}\right)}}\%$$

Numerical experiments show that this is an excellent approximation of the integral when $h>\sigma$. We may think of the requirement that $h>\sigma$ as applying to the point source case; that is, the situation where the spread about a source is small relative to the forager's reach.

Applying this approximation to the situation where there is one source at $-s$ and another at $s$ gives total benefits of

$$r_1\frac{\frac{p_0 h}{\sqrt{h^2+\sigma^2}}e^{-\frac{(x_1+s)^2}{2(\sigma^2+h^2)}}}{1+e^{\left(\frac{x_1-x_2}{h^2}\right)\left(\frac{x_1+x_2}{2}-\frac{\sigma^2x_1+sh^2}{\sigma^2+h^2}\right)}}+r_2\frac{\frac{p_0 h}{\sqrt{h^2+\sigma^2}}e^{-\frac{(x_1-s)^2}{2(\sigma^2+h^2)}}}{1+e^{\left(\frac{x_1-x_2}{h^2}\right)\left(\frac{x_1+x_2}{2}-\frac{\sigma^2x_1+sh^2}{\sigma^2+h^2}\right)}}$$

To proceed, we simplify the expression in several ways. First, we restrict our attention to the experimental situation in which $r_1$=$r_2$=$r$. Second, we drop the common factor $r\frac{p_0 h}{\sqrt{h^2+\sigma^2}}$. Third, we rewrite this expression in terms of our standard substitutions $\hat{x}_1\frac{x_1}{\sqrt{\sigma^2+h^2}}$, $\Delta=\frac{s}{\sqrt{\sigma^2+h^2}}$, and $g=\frac{\sigma^2}{h^2}$.

Finally, we introduce the computationally useful substitutions $p_i=\frac{\hat{x}_i}{\Delta}$ to obtain

$$G(p_1,p_2)=\frac{e^{-\Delta^2\frac{(p_1+1)^2}{2}}}{1+e^{\frac{\Delta^2}{2}(p_1-p_2)(p_1+p_2-g(p_1-p_2)+2)}}+\frac{e^{-\Delta^2\frac{(p_1+1)^2}{2}}}{1+e^{\frac{\Delta^2}{2}(p_1-p_2)(p_1+p_2-g(p_1-p_2)-2)}} \tag{A14}$$

This expression (A14) specifies the benefit to player 1 in terms of its position, $p_1$, and its opponent's position, $p_2$. However, the subscripts are arbitrary, so we can readily calculate the benefits to player 2, using $G(p_2, p_1)$. To find the Nash Equilibria (NE) for this game, we seek the rational reaction sets for each player. That is, we want to find player 1's best response to any player 2 choice, and player 2's best response to any player 1 choice. NE are intersections of these rational reaction sets. It is natural to begin, therefore, by seeking a $p_1$ value that maximizes $G(p_1, p_2)$ for an arbitrary $p_2$. This is a mathematically daunting task, which we can only do numerically. Using the non-competitive situation as a model, we can however find a useful characterization of the NE by exploring two special cases.

*The $p_1$=$p_2$=0 equilibria*

It is straightforward to establish that

$$\left.\frac{\partial G}{\partial p_1}\right|_{p_1=0,\,p_2=0}=0$$

so we know that $p_1$=0 is an extreme point when the opponent is at 0. To determine when this is a maximum, we consider the second derivative

$$\left.\frac{\partial^2 G}{\partial p_1^2}\right|_{p_1=0,\,p_2=0}=\frac{\Delta^2}{2}e^{\frac{\Delta^2}{2}}(-3+4\Delta^2+g)$$

The extreme at $p_1$ will be a maximum when the second derivative is negative, so we require

$3 + 4\Delta^2 + g < 0$

Solving for $\Delta^2$, we find, therefore, that there will a NE at $p_1$=0, $p_2$=0 whenever

$$\Delta^2<\frac{3}{4}-\frac{g}{4} \tag{A15}$$

*The mirror image NE*

Our situation is highly symmetric – i.e., two equivalent foragers, two equivalent sources equidistant from the center. In addition, the optimization problem revealed two coequal solutions symmetric about the center (when $\Delta$>1). We conjecture, therefore, that NE such that $p_2$=–$p_1$=$p$≠0 will exist. That is, we hypothesize the exis-

tence of non-central (non-zero) NE positions that are mirror images of one another.
To investigate this possibility we consider

$$M(p) = \left.\frac{\partial G}{\partial p_1}\right|_{p_1=p,\, p_2=p}$$

Plots of $M(p)$ show a function that has a cubic-like shape. There is always a root at $p$=0 and in some situations there is also a pair of mirror image roots at some value $\pm p \neq 0$. These mirror image roots will exist when the slope of $M(p)$ at zero is positive:

$$\left.\frac{dM}{dp}\right|_{p=0} = \frac{1}{2} e^{-\frac{\Delta^2}{2}} (-3 + 2g + 5\Delta^2) > 0$$

or when

$$\begin{aligned} -3 + 2g + 5\Delta^2 &> 0 \\ 5\Delta^2 &> 3 - 2g \\ \Delta^2 &> \frac{3}{5} \frac{2g}{5} \end{aligned} \qquad \text{(A16)}$$

We conclude that mirror image NE will exist whenever $\Delta^2 > \frac{3}{5} - \frac{2g}{5}$. Notice that the condition A15 for the existence of an NE at $p_1=p_2=0$ overlaps with the condition A16 for the existence of non-zero mirror image NE we just derived. We expect, therefore, that two NE will exist when

$$\frac{3}{5} - \frac{2g}{5} < \Delta^2 < \frac{3}{4} - \frac{g}{4}$$

*Numerical solutions*

We used numerical root-finding routines to find the non-central equilibria that are solutions of $M(p)$=0, for $\Delta^2 > \frac{3}{5} - \frac{2g}{5}$. Figure 11 shows the calculated equilibria based on these results. As in the optimization case, we see a pitchfork shape. The key difference is that here the handle of the pitchfork extends into a short central tine that represents the region where there are two NE (recall that we interpret the positive and negative tines of the pitchfork as a single equilibrium, one individual should be on the positive branch and another on the negative). The figures shows plots for a range of $g$ values.

Figure 11 shows that the non-central equilibria are similar in form to the non-central solutions we found in the individual optimization case. This suggests that an approximation similar to Eq. A9 may be appropriate. Numerical experiments show that

$$p = \pm \tanh\left(\sqrt{6\left[\Delta^2 \left(\frac{3}{5} - \frac{2g}{5}\right)\right]}\right)$$

gives an excellent approximation when $g$ is small (recall we require $g$<1). Dashed curves in Fig. 11 show this approximation.

We can, therefore, offer a reasonably complete characterization of the NE for this two-player game

$$\text{Central NE } p_1^* = p_2 = 0 \quad \text{when} \quad \Delta^2 < \frac{3}{4} - \frac{g}{4} \qquad \text{(A17)}$$

$$\text{Non-central NE } p_1 = p, p_2 = -p \qquad p \approx \tanh\left(\sqrt{6\left[\Delta^2 - \left(\frac{3}{5} - \frac{2g}{5}\right)\right]}\right)$$
$$\Delta^2 > \frac{3}{5} - \frac{2g}{5} \qquad \text{(A18)}$$

The key differences with the individual (one-player) case are (1) the non-central solutions arise at smaller source separations ($\Delta^2$=1 for the one-player case, $\Delta^2 = \frac{3}{5} - \frac{2g}{5}$ for the two-player case); (2) the non-central equilibria separate more quickly with increasing $\Delta$, and (3) central and non-central solutions exist from some parameter values in the two-player case, but not in the one-player case.

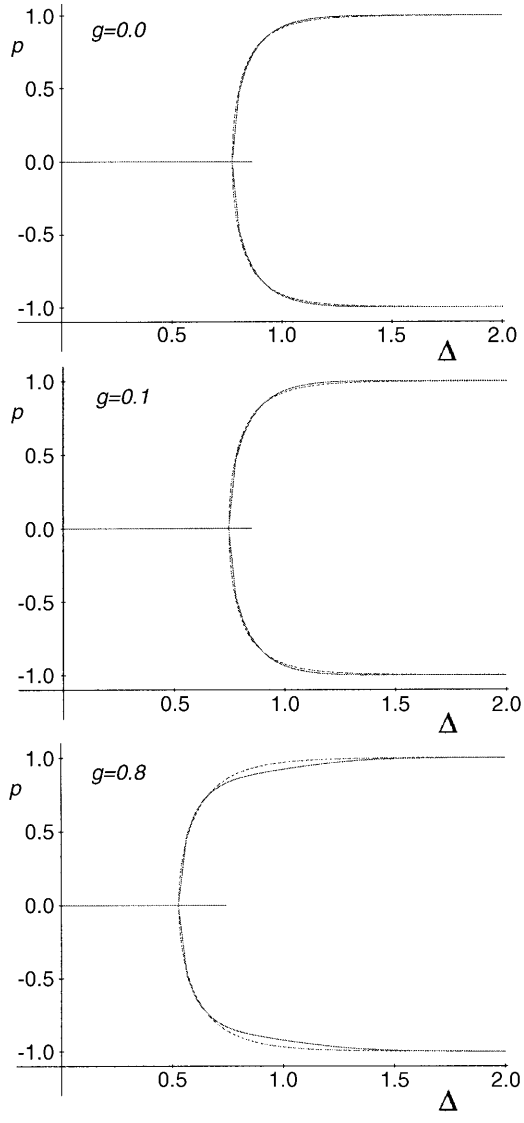


**Fig. 11** Three plots of effective source separation ($\Delta$) vs Nash equilibrium $p$-values. The *solid lines* show numerical calculated values. The *dashed lines* show the approximation A18

**Acknowledgements** We thank Sandra Knox and Jennifer Ernisse for help with the experiments. We thank Carlos Bernstein, Alex Kacelnik, Kate Lessells, Colleen McLinn, and Tom Tregenza for their comments on the manuscript. The experimental portion of this work was conducted while the authors were members of the Nebraska Behavioral Biology Group. We thank the NBBG for providing a stimulating and supportive environment. This work was supported by grant number IBN-9507668 from the National Science Foundation. This was conducted in accordance with animal use and care protocols approved by the Institutional Animal Use and Care Committee of the University of Nebraska, Lincoln.

## References

Abrahams MV (1986) Patch choice under perceptual constraints: a cause for departures from the IFD. Behav Ecol Sociobiol 10:409–415

Arditi R, Dacorogna B (1988) Optimal foraging on arbitrary food distributions and the definition of habitat patches. Am Nat 131:837–846

Bernstein C, Kacelnik A, Krebs JR (1988) Individual decisions and the distribution of predators in a patchy environment. J Anim Ecol 57:1007–1026

Bernstein C, Kacelnik A, Krebs JR (1991) Individual decisions and the distribution of predators in a patchy environment. II. The influence of travel costs and the structure of the environment. J Anim Ecol 60:205–225

Cleveland WS (1993) Visualizing data. Hobart, Summit, NJ

Fretwell SD (1972) Populations in a seasonal environment. Princeton University Press, Princeton, NJ

Fretwell SD, Lucas HL (1970) On territorial behavior and other factors influencing habitat distribution in birds. *Acta biotheoretica* 19:16–36

Gabriel W, Thomas B (1988) Vertical migration of zooplankton as an evolutionarily stable strategy. Am Nat 132:199–216

Giske J, Rosland R, Berntsen J, Fiksen O (1997) Ideal free distribution of copepods under predation risk. Ecol Model 95:45–59

Iwasa Y (1982) Vertical migration of zooplankton: a game between predator and prey. Am Nat 120:171–180

Kacelnik A, Krebs JR, Bernstein C (1992) The ideal-free distribution and predator-prey populations. Trends Ecol Evol 7:50–55

Kennedy M, Gray RD (1993) Can ecological theory predict the distribution of foraging animals? A critical analysis of experiments on the ideal free distribution. Oikos 68:158–166

Korona R (1989) Ideal free distribution of unequal competitors can be determined by the form of competition. J Theor Biol 138:347–352

Lessells CK (1995) Putting resource dynamics into continuous input ideal free distribution models. Anim Behav 49:487–494

Milinski M (1994) Ideal free theory predicts more than only input matching – a critique of Kennedy and Gray's review. Oikos 71:163–166

Mood AM, Graybill FA, Boes DC (1963) Introduction to the theory of statistics. McGraw-Hill, New York

Myers JL, Well AD (1995) Research design and statistical analysis. Erlbaum, Hillsdale, NJ

Nayfeh S (1981) Perturbation methods. Dover, New York

Parker GA, Sutherland WJ (1986) Ideal free distributions when individuals differ in competitive ability: phenotype-limited ideal free models. Anim Behav 34:1222–1242

Rosenzweig ML (1986) Hummingbird isolegs in an experimental system. Behav Ecol Sociobiol 19:313–322

Sasaki A (1997) Clumped distribution by neighborhood competition. J Theor Biol 186:415–430

Schwinning S, Rosenzweig ML (1990) Periodic oscillations in an ideal-free predator-prey distribution. Oikos 59:85–91

Sutherland WJ (1983) Aggregation and the 'ideal free' distribution. J Anim Ecol 52:821–828

Sutherland WJ, Parker GA (1992) The relationship between continuous input and interference models of ideal free distributions with unequal competitors. Anim Behav 44:345–355

Tilman D, Lehman C, Kareiva P (1997) Population dynamics in spatial habitats. In: Tilman D, Kareiva P (eds) Spatial ecology – the role of space in population dynamics and interspecific interactions. Princeton University Press, Princeton, NJ, pp 2–20

Tregenza T (1995) Building on the ideal free distribution. Adv Ecol Res 26:253–307